

Fe-Oxide/CeO₂ Composites — Magnetization Curves and Their Analyses Using the Jiles–Atherton Model

M. NIKODÝM^a, J. LUŇÁČEK^{a,*}, Y. JIRÁSKOVÁ^b, P. JANOŠ^c, J. JUŘICA^d AND O. ŽIVOTSKÝ^a

^aDepartment of Physics, VŠB — Technical University of Ostrava,
17. listopadu 2172/15, 708 00 Ostrava-Poruba, Czech Republic

^bInstitute of Physics of Materials, Academy of Sciences of the Czech Republic,
Žižkova 22, 616 62 Brno, Czech Republic

^cFaculty of the Environment, University of Jan Evangelista Purkyně,
Králova Výšina 7, 400 96 Ústí nad Labem, Czech Republic

^dRegional Materials Science and Technological Centre, VŠB — Technical University of Ostrava,
17. listopadu 2172/15, 708 00 Ostrava-Poruba, Czech Republic

The initial mixture of magnetite with 20 vol.% of cerium carbonate is treated at 673 K and 1173 K leading to formation of Fe-oxide/cerium dioxide reactive sorbents. The main interest is devoted to iron-oxide composition and interactions between both oxides mainly influencing the structural and physical magnetic properties. While the morphology did not change markedly, the transformations of initial magnetite into maghemite and/or hematite contributed to changes in magnetic properties measured at 2 K and 300 K. The magnetization curves were analysed using a theoretical Jiles–Atherton approach and discussed in connection with sorbents microstructure.

DOI: [10.12693/APhysPolA.137.601](https://doi.org/10.12693/APhysPolA.137.601)

PACS/topics: iron oxides/cerium dioxide sorbents, magnetization curves, Jiles–Atherton model

1. Introduction

CeO₂/Fe-oxide nanoparticles have been prepared for a long time due to their wide chemical applications [1, 2]. Recently, a new kind of magnetically separable reactive sorbent on the basis of the iron oxide grains and cerium dioxide nanocrystalline surface layer was developed [3]. It has been successfully tested for decomposition of a specific dangerous organophosphorus pesticide (parathion-methyl) [4] and for the chemical warfare agents soman and VX [5]. Degradation ability of the sorbents depends on the concentration of cerium dioxide and applied annealing temperature, while their magnetic properties are governed mainly by the iron oxide transformation during the calcination process [3].

This paper deals with structural and magnetic characterization and fitting of the low-temperature (2 K) and room-temperature (300 K) hysteresis loops of the sorbents by well-known isotropic Jiles–Atherton (J–A) model used for ferro/ferrimagnetic materials. Till now there are practically no results in the literature specifying relation of model parameters with loops measured on powders. The fits are introduced to 673 K and 1073 K annealed samples of iron oxide/20% cerium dioxide containing different kinds of iron oxides and thus exhibiting markedly different magnetization curves.

2. Materials and methods

2.1. Sorbents synthesis and their degradation efficiency

In this work, the original procedure for the preparation of the powder composite reactive sorbent [3] was modified. Low-cost commercially available raw materials were used for the preparation of the magnetic core. Namely, ferrous sulphate monohydrate, sold as a supplement for an animal nutrition under the name MONOSAL 30 (Precheza Přerov) served as the Fe²⁺ source, and ferric sulphate (supplied as the coagulant PREFLOC for water treatment) served as the Fe³⁺ source.

Procedure was the following. Under extensive agitation, a required amount of ferrous sulphate (MONOSAL) was dissolved in diluted sulphuric acid, and an equivalent amount of PREFLOC was added in the form of 40% solution, and finally the concentrated NaOH was added to precipitate the magnetic iron oxides. The reaction mixture was agitated for two additional hours in an inert atmosphere. Then the precipitated iron oxide (presumably magnetite) was separated with the aid of permanent magnet and washed several times with deionised water. The precipitated iron oxide was re-dispersed in the solution of cerium nitrate, and cerium carbonate was precipitated with the solution of NH₄HCO₃. The precursor was separated with the aid of permanent magnet, washed with deionised water, and dried at 383 K. Reactive sorbents were prepared by annealing the precursor at temperatures 673 K and 1073 K in an open crucible in a muffle furnace. Sorbent annealed at 673 K exhibited high degradation efficiency against parathion and paraoxon methyl being about 40% and 72%, while for 1073 K annealed sample it was only 5% and 36%, respectively.

*corresponding author; e-mail: jiri.lunacek@vsb.cz

2.2. Experimental methods

X-ray diffraction (XRD) patterns were measured at room temperature using an X'PERT PRO diffractometer with Co K_{α} radiation ($\lambda = 0.17902$ nm) in the 2θ range from 20° to 110° in steps of 0.008° and time per step 500 s. The evaluation of powder patterns was realized by the Rietveld structure refinement method [6] by semi-automatic mode using the High Score Plus program (Panalytical). Besides the phase composition, the lattice parameters and the mean crystallite size, representing a size of coherently diffracting domains, were obtained from the standard Scherrer equation. Morphology was analyzed using a TESCAN LYRA 3XMU FEG/SEM scanning electron microscope (SEM) operated at an accelerating voltage of 20 kV and equipped with an XMax80 Oxford Instruments detector for energy-dispersive X-ray (EDX) measurements. The magnetic measurements were performed using a Physical Property Measurement System (PPMS) Quantum design, Inc. The magnetization curves were taken at 300 K (RT) and 2 K (LT) in maximal magnetic field of ± 4000 kA/m.

2.3. Fitting method

For the theoretical part we used isotropic Jiles–Atherton model for simulations of the major hysteresis loops $M = f(H)$ to fit the J–A coefficients a, k, α, c by the least squares method [7]. The parameter a characterizes domain walls density in the magnetic material, k determines the hysteresis losses, α is the mean field parameter representing interdomain coupling, and c represents reversible domain wall motion [8]. The values of J–A coefficients are optimized to obtain the root square deviation r^2 (the Pearson coefficient) close to 1 showing minimal difference between the experimental and simulated magnetization curves.

3. Results and discussion

The morphology of the input magnetite/cerium carbonate mixture is seen in Fig. 1 together with X-ray diffractogram (inset top) and diffractograms of the Fe-oxide/ceria after treatments at 673 K (middle) and 1073 K (bottom), respectively. Approximately 20 vol.% in both treated states is formed by CeO_2 without any marked changes in morphology. The initial magnetite has transformed after annealing at 673 K partially into maghemite $\gamma\text{-Fe}_2\text{O}_3$ (64.6 vol.%) and after treatment at 1073 K fully into hematite. These transformations were besides the XRD confirmed by the Mössbauer spectrometry (not presented here). The lattice parameters (nm) of the CeO_2 , $a = 0.5413(5)$; Fe_3O_4 , $a = 0.8334(3)$; $\gamma\text{-Fe}_2\text{O}_3$, $a = 0.8380(5)$, $c = 0.8321(7)$; and $\alpha\text{-Fe}_2\text{O}_3$, $a = 0.5038(1)$, $c = 1.3754(3)$, fall well into values present in literature. Besides magnetite transformations the treatment temperatures have influenced the size of coherently diffracting domains that has changed from about 7 nm (CeO_2), 8 nm (Fe_3O_4), and 16 nm ($\gamma\text{-Fe}_2\text{O}_3$) to 29 nm for CeO_2 and 93 nm for $\alpha\text{-Fe}_2\text{O}_3$.

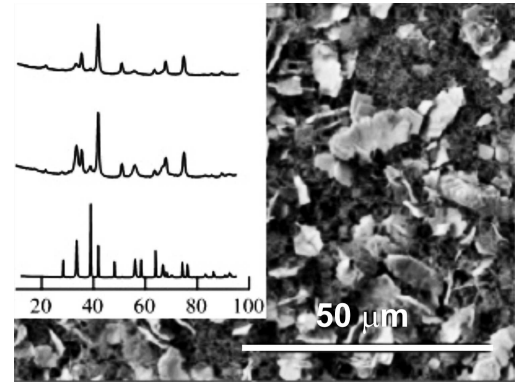


Fig. 1. Scanning electron microscope image of the input magnetite/cerium carbonate and its XRD pattern (top). Middle and bottom diffractograms correspond to Fe-oxide/ CeO_2 samples formed after annealing at 673 K and 1073 K, respectively.

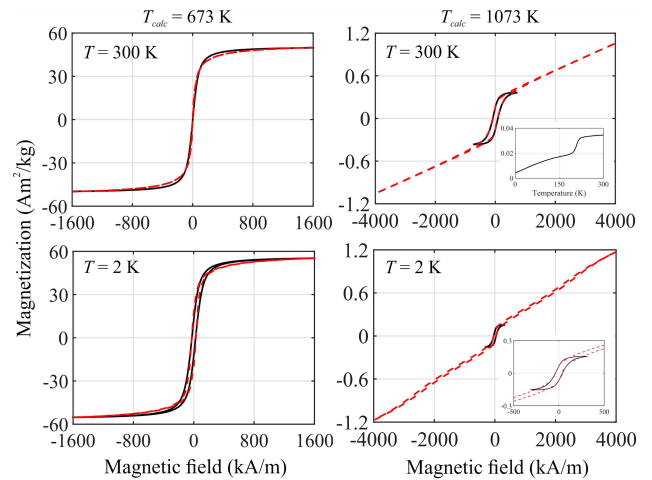


Fig. 2. Experimental (dashed red line) and fitted (solid black line) hysteresis loops at RT and LT of sorbents calcined at temperatures $T_{\text{calc}} = 673$ K (left) and 1073 K (right) (upper inset). Heating of the sample annealed at 1073 K from 2 K to 300 K (M – T curve) at constant magnetic field of 8 kA/m.

Experimental and fitted hysteresis loops measured at RT and LT for iron oxide/20% cerium dioxide samples calcinated at 673 K and 1073 K are indicated by dashed red lines and solid black lines, respectively, in Fig. 2. Measured magnetic parameters together with J–A coefficients are summarized in Table I.

RT and LT curves of 673 K calcined sample are governed by strong ferrimagnetic magnetizations of iron oxides that overlap low paramagnetic contribution of CeO_2 . Both loops have similar saturation magnetizations, while they markedly differ in the values of coercive field. Measured low value of H_c (1.71 kA/m) of 300 K loop indicates that the magnetization state is close to superparamagnetic. Fitted loops are highly sensitive to J–A coefficients a and k , while the changes of the c and α are

TABLE I

Selected magnetic parameters of iron oxide/20% cerium dioxide sorbents in dependence on the calcination temperature T_{calc} : T_{meas} — measurement temperature, H_c — coercive field, M_s — saturation magnetization ($T_{calc} = 673$ K) or saturation magnetization of ferromagnetic part ($T_{calc} = 1073$ K), M_r — remnant magnetization; a , k , α , c — coefficients of J–A model, r^2 — the Pearson coefficient

T_{calc} [K]	T_{meas} [K]	H_c [kA/m]	M_r [A m ² /kg]	M_s [A m ² /kg]	a [kA/m]	k [kA/m]	α [-]	c [-]	r^2 [-]
673	2	27.51	18.75	56.42	33.74	28.12	0.5	0.011	0.999
	300	1.71	1.78	50.69	30.112	2.96	0.5	0.004	0.999
1073	2	39.12	0.06	0.17	24.47	51.85	0.5	0.1	0.997
	300	78.15	0.16	0.41	53.67	106.04	0.5	0.1	0.996

reflected beyond the fourth and the sixth decimal place of r^2 , respectively. It is known that H_c is determined by the amount of the pinning sites and hence should correspond with the coefficient k . Surprisingly, this is fulfilled more precisely for LT loop, nevertheless, for soft magnetic materials, the condition $H_c = k$ was found [9].

The sorbent calcinated at 1073 K contains practically the same amount of CeO₂ (20.7%) and iron oxides were completely transformed to hematite known for its canted antiferromagnetic order at RT [10]. Saturation magnetization of the weakly ferromagnetic contribution at RT for the hematite nanoparticles is only between 0.21–0.29 A m²/kg and for bulk crystals it is about 0.38 A m²/kg [11], but it is still higher than paramagnetic CeO₂ contribution. This fact is reflected at measured RT loop with linear dependence of magnetization at higher fields and typical ferromagnetic reversal with high H_c at lower fields. Using the J–A model we simulated only ferromagnetic contribution of the RT loop with M_s close to mentioned observed values. Increase in a , k , and c coefficients indicating growth of the energetic losses and reversible component of the magnetization was observed with increasing calcination temperature. Measured loop at 2 K still exhibits certain ferromagnetic part, however, with lower H_c and M_s than in the case of RT loop. Simulation shows corresponding decrease of a and k coefficients, while α and c remain unchanged. Such behavior is not typical because below Morin transition (170 K–260 K [12]) the hematite should become a perfect antiferromagnet. Explanation is seen from M – T curve (upper inset of Fig. 2), when sample was heated from 2 K to RT at magnetic field of 8 kA/m. Small magnetization at 2 K comes either from not fully compensated hematite spins or from residual maghemite impurities not detected by XRD and slowly increases up to 190 K. It is followed by Morin transition finished at 225 K.

4. Conclusion

The present paper is devoted to structural and magnetic characterization and theoretical fitting of iron oxide/20% cerium dioxide reactive sorbents prepared by new procedure using the low-cost commercially available raw materials. Sorbents calcined at 673 K containing CeO₂ of nanometer size and mixture of magnetite and maghemite have optimal degradation ability to certain

toxic substances. J–A model of measured loops is sensitive to domain wall density (parameter a) and hysteresis losses (k). Sorbent annealed at 1073 K exhibits lower degradation efficiency that comes through the transformation to hematite. Here we simulate only the low ferromagnetic contribution of hematite at lower magnetic fields, while the antiferromagnetic behaviour is observed at higher magnetic fields.

Acknowledgments

This work was supported from ERDF/ESF project New Composite Materials for Environmental Applications (No. CZ.02.1.01/0.0/0.0/17_048/0007399) and from projects SP2019/26 and SP2020/45.

References

- [1] R.R. Bhosale, A. Kumar, F. AlMomani, I. Alxneit, *Ceram. Int.* **42**, 6728 (2016).
- [2] V.V. Galvita, H. Poelman, V. Bliznuk, C. Detavernier, G.B. Marin, *I&EC Res.* **52**, 8416 (2013).
- [3] P. Janoš, P. Kuráň, V. Pilařová, et al., *Chem. Eng. J.* **262**, 747 (2015).
- [4] P. Janos, P. Kuran, M. Kormunda, et al., *J. Rare Earths* **32**, 360 (2014).
- [5] K. Kim, O.G. Tsay, D.A. Atwood, D.G. Churchill, *Chem. Rev.* **111**, 5345 (2011).
- [6] *The Rietveld Method*, Ed. R.A. Young, International Union of Crystallography, Oxford University Press, Oxford 1993.
- [7] N.C. Pop, O.F. Caltun, *Acta Phys. Pol. A* **120**, 491 (2011).
- [8] D.C. Jiles, D.L. Atherton, *J. Magn. Magn. Mater.* **61**, 48 (1986).
- [9] D.C. Jiles, J.B. Thoenke, M.K. Devine, *IEEE Trans. Magn.* **28**, 48 (1992).
- [10] A.H. Morish, *Canted Antiferromagnetism: Hematite*, World Sci., 1994.
- [11] F. Bødker, M.F. Hansen, C.B. Koch, K. Lefmann, S. Mørup, *Phys. Rev. B* **61**, 6826 (2000).
- [12] Ö. Özdemir, D.J. Dunlop, *Geochem. Geophys. Geosys.* **9**, Q10Z01 (2008).